Axisymmetric slosh frequencies of a liquid mass in a circular cylinder

X. Bian, M. Perlin, W. W. Schultz, and M. Agarwal
The University of Michigan, Ann Arbor, Michigan 48109-2121

Spectral eigenvalue methods along with some lower-dimensional techniques are used to determine the natural frequencies of a liquid slug in a circular tube. The contact lines are either pinned or governed by a slip coefficient assumed small. Corresponding physical experiments are conducted for a borosilicate glass tube and a treated water slug. Gravitational and viscous effects are neglected for the analyses. The spectral results agree well with a simple spherical end cap approximation (zero dimensional) for large aspect ratio slugs and with a membrane approximation (one dimensional) for small aspect ratios. The experimental observations for different aspect ratios agree well with the predictions, although the gravity, viscosity and/or slip are neglected in the analyses. © *2003 American Institute of Physics.* [DOI: 10.1063/1.1622668]

I. INTRODUCTION

Surface wave natural frequencies with boundaries and edge constraints continue to be of much interest. Solutions to the inviscid problem with pinned contact line have been proposed.[1–5] These solutions address surface capillary and/or gravity wave applications for a layer of finite depth fluid. On the other hand the two fluid–air interfaces of a slug allow many modes that are not possible for a single interface. The problem is motivated as a first step in understanding how to move these slugs by forced vibration, possibly in microgravity.

In the analyses,[2–5] the undisturbed free surfaces are perpendicular to the solid walls. However, this is usually not the case for most applications where capillarity is important:[6,7] The fluid surfaces are highly curved in a capillary tube. Graham-Eagle[1] allows small static surface deflections and hence that analysis models the case where the apparent static contact angle is close but not equal to 90°. Motivated by nonlinear forcing of a tube and its possible fluid delivery under micro-gravity, slug motion responses are investigated by oscillating a circular cylindrical tube horizontally along its axis with a programmed periodic motion. It is thus desirable to determine the natural frequency of the end caps under pinned or partial slip contact line conditions.

Here we present a potential flow solution as a generalized eigenvalue problem by expanding the two free surfaces using Chebyshev and Fourier series with bases that satisfy continuity and impermeable wall conditions.[8] Due to surface tension, an undisturbed free surface in a circular tube is spherical in the absence of gravity. To determine the natural oscillation frequency, the dynamic and kinematic surface conditions are linearized under a small perturbation assumption and are satisfied at the undisturbed, but curved free surface.[1] Solutions are presented for slug length to diameter aspect ratios of 0.01–10. Experimental results are presented for comparison with the numerical analyses.

II. ZERO- AND ONE-DIMENSIONAL APPROXIMATIONS

As proposed by Hilpert *et al.*,[9] if the end cap remains spherically shaped for small perturbations, and the slug is long relative to the tube diameter, the inviscid slug and end cap can be modeled as a simple linear spring–mass system. An equivalent spring constant can be derived from the surface tension restoring force, inertia is determined from the center of mass motion, and then the lowest slosh frequency given accordingly. The slosh mode has primarily axial motion between two interfaces instead of the more usual particle motion for standing waves with one free surface as shown in the time lapse figure on the bottom of page 111 of Van Dyke.[10] We term this approach the end cap or the zero-dimensional (0-D) approximation (as no spatial dependent variables are required). It is apparent that for small slug length-to-diameter ratio, this method is not appropriate because flow details near the two ends are neglected. Therefore, for verification of the boundary value problem solutions, for small aspect ratios, a solution for a circular membrane (with varying thickness) vibration is included. This is valid when motion is strictly in the axial direction and the membrane tension is derived from small surface elevation. The approximation is one-dimensional (1-D) since only one spatial coordinate is required for axisymmetric solutions.

To prescribe the problem, a definition sketch and a photograph from an experiment are included in Fig. 1. All variables and parameters are scaled by the tube radius R, the density ρ, and the surface tension coefficient σ.

A. 0-D analysis: End cap approximation

The approximation is derived with the following assumptions:

(1) End caps remain spherically shaped during oscillation.
(2) A pinned condition is maintained.
(3) $L \gg R$.

The dimensionless volume V of an end cap as a function of contact angle θ is

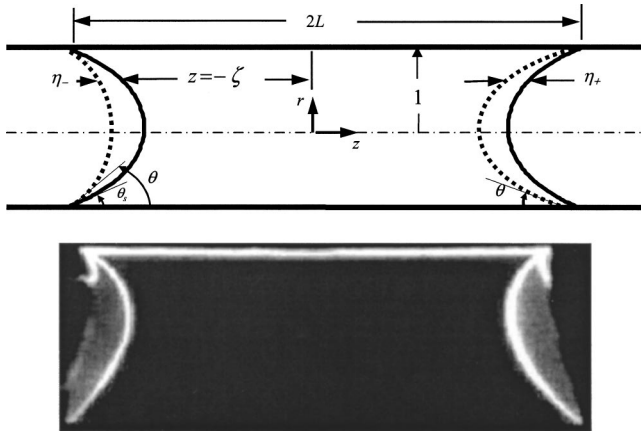3660   Phys. Fluids, Vol. 15, No. 12, December 2003

Bian *et al.*

FIG. 1. Definition sketch: Elevation view of a fluid slug with length $2L$ (well-defined for analysis with non-wetting films) and radius I in a circular cylindrical tube with pinned contact lines. $z = \pm \zeta$ (solid lines) are the undisturbed stationary surface positions and η_+ and η_- (dotted lines) are the surface perturbation relative to $\pm \zeta$, respectively. The wave analysis considered here is normally axisymmetric. This symmetry is broken by the gravitational effect on the static meniscus as shown in the photograph. Further, the wave patterns can be separated into modes where the fluid velocities or free surface disturbances $\eta_\pm$ are either even or odd. The mode sketched above is even since the deformation of both surfaces is in the same z direction. This is the lowest slosh mode and that seen predominantly in our experiments. This symmetry means that only one free surface (say η_+) needs to be considered, with the other free surface condition replaced by odd or even symmetry, and hence the $+$ or $-$ subscript is dropped. θ_s is the static contact angle. In the absence of gravity, the static free surfaces represented by $z = \pm \zeta$ are spherically shaped. θ is the apparent dynamic contact angle that oscillates in time about θ_s. The photo at the bottom is from a Kodak high-speed imager where the slug is illuminated by a vertical laser sheet through the slug axis. To increase the image contrast, the water slug is fluorescein treated, decreasing the static surface tension by approximately 3.5 dyn/cm (Ref. 12).

$$V(\theta) = \frac{\pi}{3} \frac{\cos \theta (2 + \sin \theta)}{(1 + \sin \theta)^2}.$$

The derivative of the volume with respect to the contact angle is

$$\frac{\partial V}{\partial \theta} = -\pi \frac{1}{(1 + \sin \theta)^2}.$$

Considering the right side surface in Fig. 1, the small center of mass displacement with respect to equilibrium θ_s is

$$\Delta z = -\frac{\partial V(\theta_s)}{\partial \theta} \frac{\Delta \theta}{\pi}.$$

The pressure change by surface tension due to a small end cap perturbation $\Delta \theta = \theta - \theta_s$ is

$$\Delta p = 2(\cos \theta - \cos \theta_s) \cong -2 \sin \theta_s \Delta \theta$$

$$= -2 \sin \theta_s (1 + \sin \theta_s)^2 \Delta z.$$

The total restoring force and the equivalent spring constant K_{eq} from both menisci are determined from

$$\Delta F = 2\pi \Delta p = -4\pi \sin \theta_s (1 + \sin \theta_s)^2 \Delta z = -K_{eq} \Delta z.$$

Thus the natural angular frequency for the mass–spring system is

$$\omega^2 = \frac{K_{eq}}{m} = \frac{4\pi \sin \theta_s (1 + \sin \theta_s)^2}{m},$$

where $m = 2\pi L$ is the mass of the slug when neglecting the small volume in the end caps and L is the length-to-diameter aspect ratio. Thus the natural frequency in nondimensional form is

$$\omega^2 = \frac{2 \sin \theta_s (1 + \sin \theta_s)^2}{L}. \tag{1}$$

B. 1-D approximation: Membrane approximation

For a sufficiently short slug with a flat (or a nearly flat) free surface, flow can be reasonably assumed to be parallel to the axial direction. The dynamic governing equation for axisymmetric surface motion is 1-D. The undisturbed free surfaces are $z = \pm \zeta$ where

$$\zeta = L + \tan(\theta_s) - \sqrt{\sec^2 \theta_s - r^2}. \tag{2}$$

The surface perturbation is η. The pressure jump across the interface is determined by the surface tension times surface curvature (the independent variable subscripts refer to partial differentiation):

$$\frac{\Delta p}{\sigma} = \frac{s_{rr} + \eta_{rr}}{[1 + (s_r + \eta_r)^2]^{3/2}} + \frac{s_r + \eta_r}{r\sqrt{1 + (s_r + \eta_r)^2}}$$

$$\approx \frac{s_{rr}}{[1 + s_r^2]^{3/2}} + \frac{\eta_{rr}}{[1 + s_r^2]^{3/2}} - 3\frac{s_r s_{rr} \eta_r}{[1 + s_r^2]^{5/2}}$$

$$+ \frac{s_r}{r\sqrt{1 + s_r^2}} + \left(\frac{1}{r\sqrt{1 + s_r^2}} - \frac{s_r^2}{r(1 + s_r^2)^{3/2}} \right) \eta_r,$$

where the approximation derives from small η, η_r, and η_{rr}. Considering both surfaces, we linearize the dynamic equation for the membrane about its spherical surface:

$$\frac{\eta_{rr}}{(1 + s_r^2)^{3/2}} + \left[\frac{1}{r\sqrt{1 + s_r^2}} - 3\frac{s_r s_{rr}}{(1 + s_r^2)^{5/2}} - \frac{s_r^2}{r(1 + s_r^2)^{3/2}} \right] \eta_r$$

$$= \zeta \eta_{tt}. \tag{3}$$

This non-constant coefficient wave equation can be solved numerically (i.e., constructing η as a summation of polynomials or trigonometric functions in r and harmonic in time t) for frequencies and modes. When the surface is flat we have the standard membrane equation

$$\nabla^2 \eta = L \eta_{tt}.$$

The axisymmetric normal modes of this boundary value problem are

$$\eta = J_0(\omega_n \sqrt{L} r) \cos \omega_n t, \quad n = 1, 2, 3, ...,$$

where J_0 is the zeroth-order Bessel function of the first kind. The pinned boundary condition results in the eigenequation $J_0(\omega_n \sqrt{L}) = 0$. The lowest slosh frequency is

$$\omega_1 \approx \frac{2.405}{\sqrt{L}}. \tag{4}$$

III. THE COMPLETE INVISCID BOUNDARY VALUE PROBLEM AND ITS LINEARIZATION

Assuming an inviscid flow, the problem may be formulated under the following conditions and additional assumptions:

(a) Irrotational flow.
(b) No-flow through the cylinder walls.
(c) Linearized free surface boundary conditions.
(d) Spherical undisturbed free surface in the assumed absence of gravity.
(e) Pinned contact lines along each of the two free surfaces.

To determine the natural frequencies and mode shapes of the ends of the slug, the associated equations are formulated as a generalized eigenvalue problem. The two surface elevation perturbations relative to the unperturbed curved surfaces $z = \pm \zeta(r)$ are expanded as a summation of basis functions (cosine series, Chebyshev polynomials, etc.).

In cylindrical coordinates, the equations governing the fluid are simply

$$\nabla^2 \Phi = 0, \tag{5a}$$

$$v(r=1,t) = \frac{\partial \Phi}{\partial r} = 0, \tag{5b}$$

where Φ is the velocity potential and v is the radial velocity. Only one of the surfaces $z = \zeta(r)$ as shown in Fig. 1 needs to be considered due to symmetry (or antisymmetry). Eliminating the static equilibrium terms, the dynamic and kinematic surface boundary conditions for the linearized axisymmetric free surface (η_+) are

$$\frac{\eta_{rr}}{(1+s_r^2)^{3/2}} + \left[\frac{1}{r\sqrt{1+s_r^2}} - 3\frac{s_r s_{rr}}{(1+s_r^2)^{5/2}} - \frac{s_r^2}{r(1+s_r^2)^{3/2}} \right] \eta_r$$

$$= \Phi_t,$$

$$\frac{\partial(\zeta+\eta)}{\partial t} + \frac{\partial \Phi}{\partial r}\frac{\partial(\zeta+\eta)}{\partial r} = \frac{\partial \Phi}{\partial z} \Rightarrow \eta_t \approx \Phi_z - \zeta_r \Phi_r,$$

$$\eta = 0 \quad (r=1). \tag{6}$$

IV. NUMERICAL SOLUTION OF THE BOUNDARY VALUE PROBLEM

A general solution to the boundary value problem (5a) and (5b) is

$$\Phi = e^{i\omega t} \sum_{n=0}^{\infty} \sum_{m=0}^{\infty} \left(A_{mn} \frac{\cosh k_n z}{\cosh k_n L} \right.$$

$$\left. + B_{mn} \frac{\sinh k_n z}{\sinh k_n L} \right) \cos m\psi \frac{J_m(k_n r)}{J_m(k_n)}, \tag{7}$$

where J_m represents the Bessel function of the first kind of the mth order and k_n are the zeros of J_m' to satisfy the wall condition (5b). Here, ψ is the polar angle and m is the azimuthal wavenumber. The $e^{i\omega t}$ term indicates a solution har-
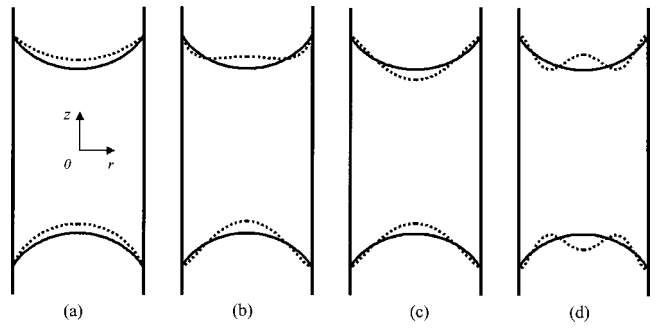

FIG. 2. Lowest modes for $L=10$ with static contact angle $\theta_s = 40°$. The resulting frequencies ω are 0.598 41, 8.324 488, 8.324 486, and 18.172 226, respectively. We consider (a) to be the fundamental slosh mode and it is the primary focus of the discussions. The 0-D approach applies to (a) only.

monic in time. For axisymmetric solutions, $m=0$, we remove the first subscript of A_{mn} and B_{mn} for simplicity. Separating to even and odd cases in z yields

$$\Phi_1 = e^{i\omega t} \sum_{n=0}^{\infty} A_n \frac{\cosh k_n z}{\cosh k_n L} \frac{J_0(k_n r)}{J_0(k_n)}, \tag{8}$$

and

$$\Phi_2 = e^{i\omega t} \sum_{n=0}^{\infty} B_n \frac{\sinh k_n z}{\sinh k_n L} \frac{J_0(k_n r)}{J_0(k_n)}. \tag{9}$$

Φ_1 represents a solution with zero axial velocity at $z=0$ as if there were a solid wall there (see Fig. 2 modes c and d) and Φ_2 represents the slosh mode only realizable for a slug (two free surfaces condition). For a given static contact angle θ_s, ζ is prescribed according to the spherical static shape. Using a Fourier series to describe the surface elevation in harmonic motion yields

$$\eta = e^{i\omega t} \sum_{n=1}^{N} c_n \cos j_n r, \quad j_n = (n-1/2)\pi, \quad n=1,2,3,... \tag{10}$$

or with Chebyshev polynomials:

$$\eta = e^{i\omega t} \sum_{n=1}^{N} c_n \phi_n(r), \quad \phi_n(r) = T_{2n}(r) - 1, \quad n=1,2,3,.... \tag{11}$$

Both automatically satisfy $\eta_r(r=0)=0$ and $\eta(r=1)=0$ for the axisymmetric mode.

A generalized eigenvalue problem is posed by (6) and (8) or (9) upon using (10) or (11). Calculations are conducted for aspect ratios of 0.01 to 10. Since the basis functions satisfy the equations in the domain and on the side walls, the solution is obtained by collocation on the free surface. We use standard collocation points:[11] evenly spaced in r for the Fourier expansion (10) and zeroes of the Chebyshev polynomials for the Chebyshev expansion (11). The collocation points were placed on the curved, but unperturbed surfaces. When we used N collocation points to obtain the algebraic eigenvalue system, our eigenvalue was reasonable for modest values of N but diverged for larger N. Examination of the boundary conditions showed large oscillatory residuals between the collocation points near $r=0$ for the Chebyshev

TABLE I. Convergence test with Chebyshev and Fourier surface expansions for different static contact angle for lowest mode when $L=10$. "—" indicates no real eigenvalue is calculated for the lowest mode. Convergence for smaller θ_s becomes problematic, but then viscous effects enter to make the physical model invalid.

	$\theta_s=20°$		$\theta_s=30°$		$\theta_s=45°$		$\theta_s=65°$		$\theta_s=90°$	
N	Chebyshev	Fourier	Chebyshev	Fourier	Chebyshev	Fourier	Chebyshev	Fourier	Chebyshev	Fourier
10	0.361 479	—	0.484 132	—	0.650 763	0.679 158	0.815 895	0.816 924	0.891 566	0.887 974
20	0.359 978	—	0.484 134	—	0.650 763	—	0.815 898	0.816 443	0.983 437	0.890 041
50	0.359 977	—	0.484 134	—	0.650 763	—	0.815 907	—	—	0.890 630
100	0.359 977	—	0.484 134	—	0.650 763	—	0.815 902	—	—	0.890 721

expansion and near the contact line $(r=1)$ for the Fourier expansion. Numerical experiments showed that using $1.5N$ collocation points to obtain an overdetermined system drastically reduced these errors and allowed convergence for large N when Chebyshev expansion was used, but no similar improvement was found for the Fourier expansion. Singular value decomposition was then used as the solver for the overdetermined system. The collocation procedure is nonstandard in that the free surfaces are not coordinate surfaces, but we recover the results of Henderson and Miles[2] when only one free surface is present and the undisturbed surface is flat. Our attempts at using a Galerkin method did not converge.

The generalized spectral eigenproblem is singular. When kinematic and dynamic surface conditions are combined into a single equation as a general eigenvalue problem, inverted differential operators are needed. Spurious eigenvalues and slow convergence are thus possible (Boyd,[11] pp. 139–142).

The Fourier series numerical solutions for static contact angle θ_s close to 90° converge rapidly, while scaling and roundoff errors accumulate. However, for θ_s near 90°, the Chebyshev polynomials fail to converge before spurious eigenvalues (with paired imaginary frequencies) dominate the solutions. Interestingly for smaller θ_s, the Chebyshev polynomials converge while the Fourier expansions do not converge, as shown in Table I. Both expansions exhibit convergence difficulties for small θ_s (approximately 20° and below). This may be caused by the physically sharpened corner singularity and increased condition numbers of the resulting linear algebraic system (considering the exponential expansion in the axial direction). It is not clear why the two

expansions exhibit different convergence for different θ_s regions. A global convergent solution for all static contact angles may necessitate a different series or a combined strategy.

V. RESULTS AND COMMENTS

In Table II, numerical results are presented along with the 0-D and 1-D approximations for different aspect ratios. As expected from the discussion in Sec. II, the potential solution converges to the 1-D approximation for small aspect ratio (see $L=0.01$, $\theta_s=90°$), and appears to converge to the 0-D approximation for large aspect ratio ($L=10$). The 15% difference between the 0-D solution and the other approximations in the $L=0.01$, $\theta_s=90°$ case is caused by the non-spherical shape of the slug in the membrane limit.

The four lowest 2-D modes are presented in Fig. 2 for $L=10$, now with static contact angle $\theta_s=40°$ Only the axisymmetric modes are considered. As expected, the fundamental slosh mode [Fig. 2(a)] has the lowest frequency. One [Fig. (2b)] is also even in η. The other two modes have odd perturbations and the flow behaves as if there were a solid wall at $z=0$ (Faraday waves[2]). It is also apparent that for $L=10$ the second and third modes in Fig. 2 have very similar frequencies. This is as expected for similar surface modes of slugs with large aspect ratio: The relation between the two surfaces is weakened by a large mass between them (with the obvious exception of the fundamental slosh mode). Thus the two surfaces behave somewhat independently, leading to similar flow fields for the two modes.

TABLE II. Pseudospectral results, nondimensional lowest frequencies ω, show convergence to 0-D approximation for $L=10$ and convergence to 1-D approximation for $L=0.01$.

		$L=0.01$		$L=0.1$		$L=1$		$L=10$	
θ_s		90°	89°	90°	80°	90°	30°	90°	30°
0-D approximation: (spherical end cap)		28.2843	28.280 00	8.9443	8.8086	2.828 43	1.5	0.8944	0.4743
1-D approximation (membrane)		24.0500	41.531 52	7.6053	12.9810	2.4050	1.8250	0.7605	0.4476
Spectral method for varying truncation N	100	24.0506	41.535 91	7.6680	13.0890	2.7138	1.9376	0.8907	0.4841
	50	24.0506	41.534 11	7.6680	13.0890	2.7140	1.9376	0.8906	0.4841
	20	24.0508	41.521 77	7.6685	13.0873	2.7155	1.9376	0.8880	0.4841
	5	24.0871	41.324 34	7.6839	13.0488	2.7522	1.9532	0.8803	0.4890
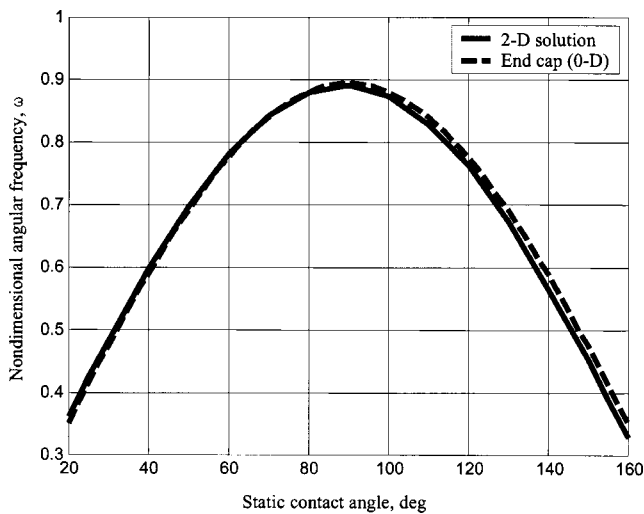
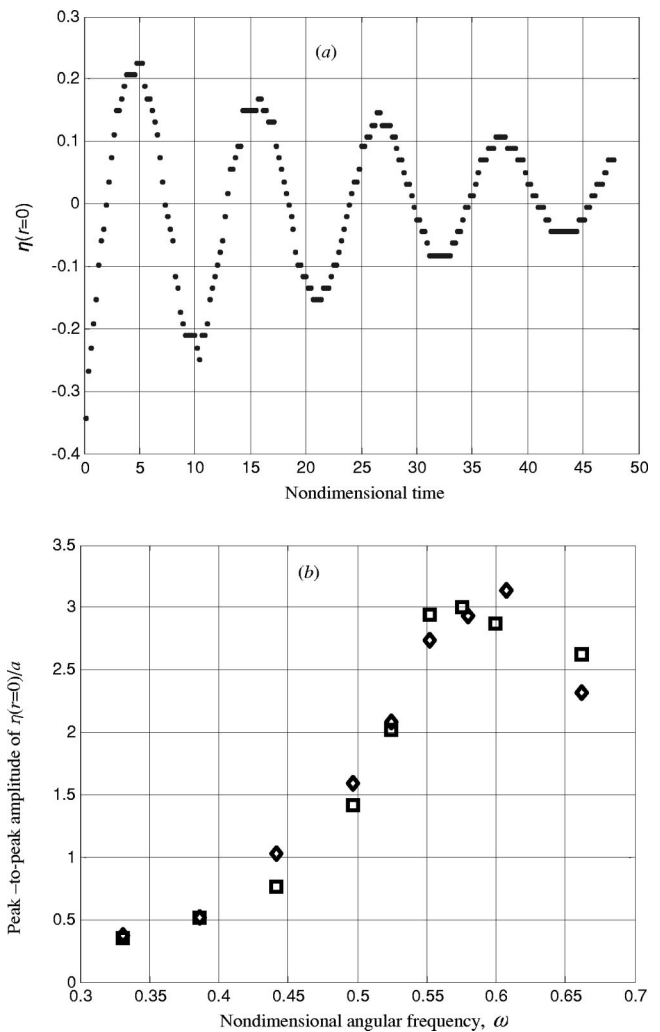FIG. 3. Lowest slosh frequency vs static contact angle for $L=10$.

FIG. 4. Free and forced oscillations experimentally determine the natural frequency of a water slug in a cylindrical tube with pinned contact line and a nearly spherical end cap. (a) The tube is suddenly stopped from constant velocity while recording the surface elevation $\eta(r=0)$. A natural frequency of 0.571 fits the data in the figure. (b) The tube is driven horizontally by a harmonic displacement $x=a\cos\omega t$ where $a\omega^2$ is held constant and a is sufficiently small to be in the linear regime (we used $a=0.15$ for $\omega=1.104$). The peak-to-peak amplitude of the surface elevation (normalized by a) is plotted as a function of ω for two replicated experiments. The open square shows a maximum resonance at 0.575, while the open diamond shows a maximum resonance at 0.610. The difference is 6% between the two experiments. The tube diameter is $D=3.556$ mm, and the aspect ratio L is 10. HPLC grade water is used within a borosilicate glass precision ground tube.

Figure 3 presents results of the potential and the 0-D solutions for varying θ_s and for fixed large aspect ratio $L=10$. The 2-D results shown in Fig. 3 are given for Chebyshev or Fourier expansions in favor of convergence. According to (1), the frequency for the 0-D approximation is symmetric with respect to $\theta_s=90°$.

For comparison with numerical results, free oscillation and forced oscillation tests were conducted. A precise borosilicate glass tube was used with internal diameter $D=3.556$ mm and square outer cross section 12.7 mm $\times$ 12.7 mm for reduced optical distortion. The tube was washed with alcohol and HPLC grade water, and then dried with dry compressed air. The liquid slug was made using HPLC grade water. For the free oscillation test, the tube motion was stopped suddenly from a constant horizontal speed and the end cap apex position as a function of time was recorded by a Kodak high speed video imager; the results are presented in Fig. 4. The time origin in Fig. 4(a) was chosen after a sufficient time to avoid initial transients, contact line slip, and nonlinearity. To measure the contact angle, the interface was assumed to be spherically shaped and the height of the end cap was taken as the average horizontal distance from the upper and lower contact line in a 2-D image to that at the apex. (Similar measurements fitting a circle to the two contact line locations and the apex produced similar results with more experimental error.) Presumably due to contact line hysteresis, the initial contact angles were measured as approximately $30°–70°$ when the slug was placed in a dry tube by syringe.

We found less experimental scatter when an initial disturbance was sufficiently large to cause slip motion—slip caused by other forces generally had a similar effect. The static contact angle measured immediately following the free oscillation decay generally had a scatter of $\pm5°$. No dependence on aspect ratio was observed for the range we measured ($1.28\le L\le10.3$). For the forced oscillation test, the tube was driven horizontally by a harmonic displacement $x=a\cos\omega t$, where the forcing amplitude $a\omega^2$ was held constant. Thus the amplitude of the end cap motion as a function

of frequency was obtained and is plotted in Fig. 4(b). In both experiments, the pinning of the contact line was ensured by constantly monitoring contact line motion relative to the tube.

We found that the free oscillation test is simpler to control. Only one experiment is required for a given slug to estimate the natural slosh frequency, and the actual static contact angle can be obtained immediately following the end cap displacement measurement. On the other hand, the forced oscillation requires measurements for different frequencies and the slug will often slip near the resonant frequency. Due to contact line hysteresis, it is difficult to have the same contact angle for replicated experiments. The mea-
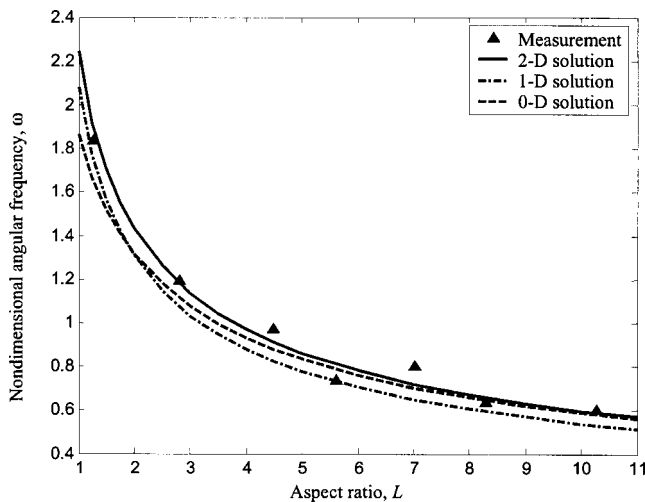
FIG. 5. Natural slosh frequencies by measurement, 2-D, 1-D, and 0-D approach for different aspect ratio. The contact angle used for prediction is 40° determined according to the measurement procedure described in the text.

FIG. 6. Lowest slosh frequency vs the slip parameter γ, defined as the slip coefficient in the contact line stick-slip condition at $r=1$: $\eta + \gamma \eta_r = 0$, where η is the surface perturbation from the curved static free surface. $L = 10$ and $\theta_s = 40°$.

sured natural frequencies for different aspect ratio are presented in Fig. 5 together with the 0-D, 1-D, and 2-D approaches. The contact angle used for prediction, θ_s, is 40° according to the measurement in Sec. V.

Even for potential flow, a trijunction singularity exists when the free surface is not perpendicular to the solid. The analyses demonstrate that for a pinned contact line liquid slug with large length-to-diameter ratio L, the potential flow solution and the end cap approximation are in agreement. The analyses also agree well with the experimental results although the gravity effect and viscous dissipation are neglected. This indicates that for a long, pinned, inviscid slug the inner flow may be neglected when determining the resonance of the end cap. The restoring force in the end cap (0-D) model is contact angle variation—while curvature remains constant over the entire surface when gravity is negligible.

APPENDIX: EFFECT OF SLIP

A stick-slip boundary condition for the contact line is implemented and its results are shown in Fig. 6. Although experimental slip conditions for this case are more complicated,[12] we use a simple stick-slip contact line model that is similar to Hocking[13] (i.e., $\eta + \gamma \eta_r = 0$ on $r=1$). As $\gamma \to 0$, the frequencies converge to the pinned contact-line
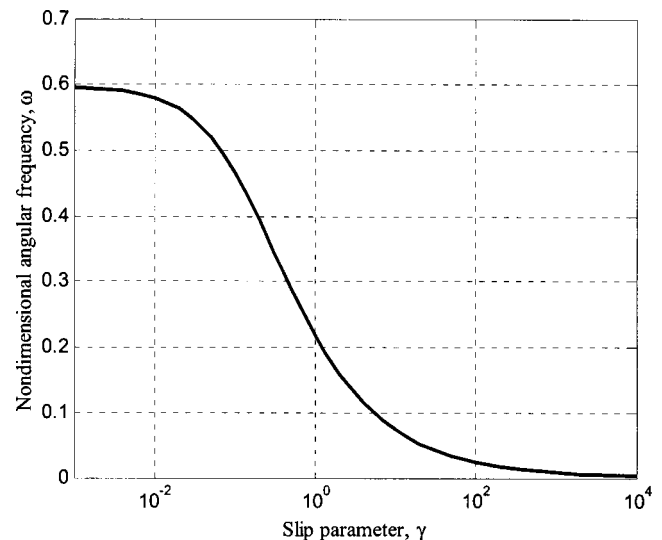
solution (about 0.6 in Fig. 3 for $\theta_s = 40°$). As $\gamma \to \infty$, the contact line slips on the wall boundary, and the frequency goes to zero as the restoring force of the meniscus vanishes.

[1] J. Graham-Eagle, "A new method for calculating eigenvalues with applications to gravity-capillary waves with edge constraints," Math. Proc. Cambridge Philos. Soc. **94**, 553 (1983).
[2] D. M. Henderson and J. W. Miles, "Surface-wave damping in a circular cylinder with a fixed contact line," J. Fluid Mech. **275**, 285 (1994).
[3] J. Wright, S. Yon, and C. Pozrikidis, "Numerical studies of two-dimensional Faraday oscillations of inviscid fluids," J. Fluid Mech. **402**, 1 (2000).
[4] H. F. Bauer, "Coupled frequencies of a frictionless liquid in a circular cylindrical tank with an elastic partial surface cover," J. Sound Vib. **230**, 1147 (2000).
[5] H. F. Bauer, "Response of an anchored viscous liquid layer to axial excitation in zero-gravity," Z. Angew. Math. Mech. **74**, 369 (1994).
[6] E. Ramé, "On an approximate model for the shape of a liquid–air interface receding in a capillary tube," J. Fluid Mech. **342**, 87 (1997).
[7] C. Martel, J. A. Nicolas, and J. M. Vega, "Surface-wave damping in a brimful circular cylinder," J. Fluid Mech. **360**, 213 (1998).
[8] H. N. Oguz and A. Prosperetti, "The natural frequency of oscillation of gas bubbles in tubes," J. Acoust. Soc. Am. **103**, 3301 (1998).
[9] M. Hilpert, D. Stopper, and G. H. Jirka, "Resonance of a liquid column in a capillary tube," Z. Angew. Math. Phys. **48**, 424 (1997).
[10] M. Van Dyke, *An Album of Fluid Motion* (Parabolic, Stanford, CA, 1982).
[11] J. P. Boyd, *Chebyshev and Fourier Spectral Methods*, 2nd ed. (Dover, Mineola, NY, 2000).
[12] C. Ting and M. Perlin, "Boundary conditions in the vicinity of the contact line at a vertically oscillating upright plate: An experimental investigation," J. Fluid Mech. **295**, 263 (1995).
[13] L. M. Hocking, "Waves produced by a vertically oscillating plate," J. Fluid Mech. **179**, 253 (1987).